

RF CHARACTERISTICS OF HIMAC INJECTOR LINAC

K. Sawada, S. Hara, K. Okanishi, H. Murata, T. Sakata, O. Morishita, S. Yamada*, A. Kitagawa*, Y. Sato*, H. Ogawa*, and Y. Hirao*

Sumitomo Heavy Industries, LTD.

5-2 Soubiraki-cho, Niihama-shi, Ehime 792

* National Institute of Radiological Sciences

4-9-1 Anagawa, Chiba 260

Abstract

Almost all of the accelerator components for the HIMAC injector are fabricated and the performance tests are in progress in accordance with the schedule of installation to the NIRS site in March 1992. For the Alvarez linac which is the main part of the HIMAC injector, a test for RF characteristics of the first cavity had been already done at the clean shop of SHI (Sumitomo Heavy Industries, LTD.) a year ago. A satisfactory performance was confirmed. Tests and tuning on the remaining cavities and other accelerator parts are in progress.

Introduction

The HIMAC (Heavy Ion Medical Accelerator in Chiba) injector consists of PIG and ECR ion sources, an RFQ linac, an Alvarez linac, beam transport lines, RF sources, various power supplies and so on. Figure 1 shows the layout of the injector and table 1 lists the main parameters. Beams are extracted from the PIG or ECR source at the energy of 8 keV/u and with charge to mass ratio larger than or equal to 1/7. They are injected into the RFQ linac through the beam transport line. The RFQ linac accelerates the beams to the energy of 800 keV/u, and the Alvarez linac, which consists of three cavities, increases the energy up to 6 MeV/u. The output beam from the Alvarez linac passes through a carbon foil to increase the charge state of the heavy ions and is injected into a synchrotron ring after the momentum spread reduced to less than 0.3 % by a debuncher cavity.

Almost all of the accelerator components are fabricated and their performance tests are under way. For the 2 types of the ion sources, sufficient beam intensities and stable operation are already realized for ion species such as He, C, Ne, Si, and Ar.^{(1) (2)} The RFQ linac is in the stage of vane alignment at present. Fabrication of the no.3 tank of the Alvarez linac had been finished and the test for RF characteristics had been done about a year ago. For the test, consisting of the tuning of acceleration field and resonant frequency, breakdown test at high RF power operation and performance test of RF control circuits, satisfactory results were obtained. For the no.2 tank of the Alvarez linac, tuning of acceleration field and resonant frequency has been also finished and the high RF power operation are under preparation. The no.1 tank is being subjected to alignment of the drift tubes, and its RF test will be started soon. Measurements of excitation characteristics and magnetic field distribution for the various elements of the beam transport lines such as quadrupole magnets, bending magnets, and solenoid magnets, were completed and the results were found to satisfy the design objectives. Profile, emittance, and electrostatic bunch monitors are under fabrication and the performance measurement will be done after the monitors will become available for tests.

This paper describes the design of the Alvarez cavities and the RF system as well as the results of the test for the RF characteristics performed at the SHI clean shop.

Table 1
Specification for the HIMAC injector

Input energy for RFQ linac	8 keV/u
Output energy for RFQ linac	800 keV/u
Output energy for Alvarez linac	6 MeV/u
RF pulse width	1.2 msec
RF repetition rate	3 Hz max.
RF frequency	100 MHz
Charge to mass ratio	1/2 - 1/7

Table 2
Main parameters for Alvarez linac

No. of tank	1	2	3
Synchronous phase (deg)	-30	-25	-25
Output energy (MeV/u)	2.669	4.385	6.060
Cell no.	56	28	22
Tank length (m)	9.768	7.202	6.907
Tank diameter (m)	2.20	2.18	2.16
Bore radius (cm)	1.0	1.5	1.5
Theoretical Q value	120000	124000	126000
Acceleration field (MV/m)	1.808	2.102	2.102
Maximum field (MV/m)	9.79	12.34	12.84

Cavity design

Table 2 shows main parameters for the Alvarez linac. The linac consists of 106 cells in the 3 cavities. Each drift tube is supported by two stems and aligned in the cavities. Each tank has three types of tuners named "fixed-tuner", "manual-tuner", and "auto-tuner". The fixed-tuners are used for initial tuning of the acceleration field and the resonant frequency by varying the projection volumes inside the cavity. After the tuning, they are fixed. The manual-tuners are for fine tuning of the field and the frequency. The auto-tuners are used to compensate for the frequency drift during operation. The no.1 tank has 9 fixed-tuners, 2 manual-tuners, and 2 auto-tuners. The no.2 and no.3 tank have 6 fixed-tuners, 2 manual-tuners, and 2 auto-tuners each. RF power required for the design acceleration field are 970 kW for the no.1, 930 kW for the no.2, and 860 kW for the no.3 tank, assuming 70 % Q value of that calculated for perfect copper conductor. A dedicated RF chain for each cavity feeds the power through a single loop coupler.

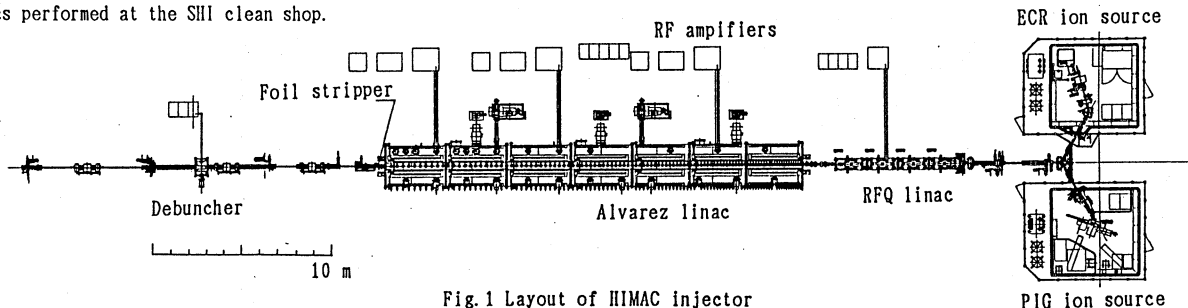


Fig.1 Layout of HIMAC injector

RF system design

Figure 2 shows the RF system block diagram. Three RF chains drive the three Alvarez cavities separately. Each RF chain contains RF control circuits (AGC and APC), a transistor amplifier, and three stages of amplifiers using tetrode tubes. Low level 100 MHz from a signal generator is amplified up to 1.5 MW maximum through the chain and fed to the cavities.

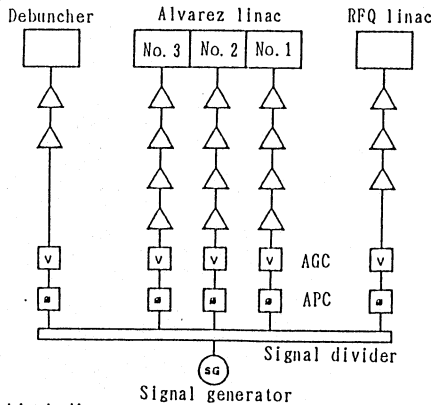


Fig. 2 RF system block diagram

RF amplifiers

Table 3 shows the design parameters of the tetrode tube amplifiers. The maximum power for each stage is 7.5 kW, 130 kW, and 1.5 MW, respectively. The 1st and 2nd stages are of granded-grid types and the final stage is in a granded-cathode configuration.

Figure 3 shows the schematic drawing of the final stage amplifier. The amplifier has a single ended coaxial structure composed of three kinds of resonators, which are used for the input, G1-G2, and output channels. These resonators have RF terminals at the lower end which are the movable plungers to tune the resonant frequencies, so that the tetrode tube is located at the top. The input and output resonators resonate in $3/4\lambda$ modes and the G1-G2 in a $1/4\lambda$ mode. Coaxial lines of 120D and 203D are used for input and output transmission lines. Loops are used as couplers between the resonators and the coaxial lines. The coupling strength is optimized by adjusting the azimuthal angle of the loop with respect to the field direction inside the resonator.

Table 3
Design parameters of the tetrode tube amplifiers

Step no.	1st	2nd	Final
Tube type	RS2032CL	RS2058CJ	RS2074SK
Input power	0.03 kW	6.2 kW	110 kW
Output power	7.5 kW	130 kW	1500 kW
Plate voltage	6.5 kV	10 kV	20 kV
Screen voltage	0.8 kV	1 kV	1.5 kV
Grid voltage	140 ± 15 V	255-315 V	630-690 V
Plate current	1.7 A	18.5 A	101 A
Plate loss	3.5 kW	61 kW	610 kW
Efficiency	68 %	70 %	74 %
Load impedance	2000 Ω	310 Ω	120 Ω

RF control circuit

RF control circuits are composed of AGC (Automatic Gain Controller), APC (Automatic Phase Controller), and AFC (Automatic Frequency Controller). AGC and APC control the RF amplitude and phase in the cavity, and AFC keeps the resonant frequency constant by varying the insertion depth of the auto-tuners in the cavity.

Figure 4 shows the block diagram of the AGC and APC. Signals containing RF amplitude and phase information inside each cavity picked up by a loop monitor are fed to an error amplifier and are compared with the preset reference values supplied from the UDC (Universal Device Controller). Signals generated there modify the gain or phase in the RF chain. This feedback system has an enough fast time constant so that the control can be done within

the RF pulse duration of 1.2 msec.

Figure 5 shows the block diagram of the AFC. The circuit compares the RF phase of a signal from a loop monitor with that of the forward power from the final stage amplifier. The phase difference represents a shift of the resonant frequency from the excitation frequency. A signal proportional to the frequency difference is generated and moves the auto-tuners during the intervals between RF pulses to compensate for the resonant frequency drift of the cavity.

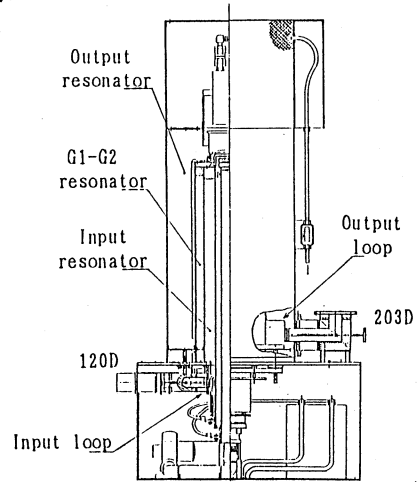


Fig. 3 Schematic drawing of the final stage amplifier.

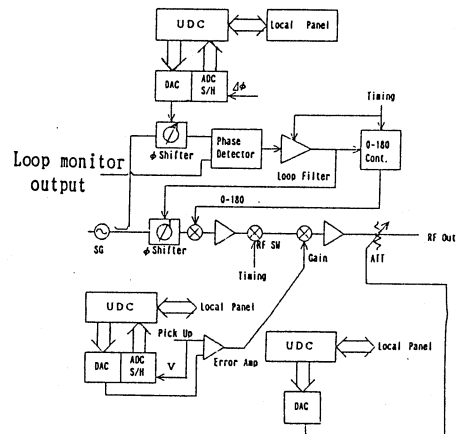


Fig. 4 Block diagram of the AGC and APC.

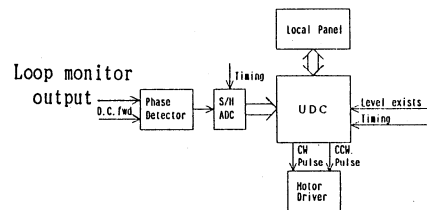


Fig. 5 Block diagram of the AFC.

Tuning of Acceleration field and resonant frequency

Electrical field along the beam axis was measured with a perturbation method. In fig. 6, stepped figure shows a typical result of the field measurement for the 90th cell and a full line shows the field distribution calculated by the 'SUPERFISH' code. Good agreement between the two assures reliability of the measurement. After repeating field measurements through a cavity axis and adjustments of the fixed tuners under an atmospheric condition, flat field distributions shown in fig. 7 for the no. 2 and fig. 8 for the no. 3 tank were obtained at 99.97 MHz. Field uniformity is obtained within 3.5 % for the no. 2 and 3 % for the no. 3 tank. Effect of non-uniformity of this level is negligible for beam acceleration.

High RF power operation

By the high RF power operation, RF power was fed with repetition rate of 3 Hz and width of 1.2 msec to the no.3 tank after connection of the RF chain was completed. RF power of 1.5 MW maximum was obtained from the final stage amplifier and full power operation was conducted. The design value of the maximum surface field for the cavity is 12.84 MV/m (Kilpatrick coefficient is 1.13), and the Q value measured after the operation was 102,000 (81 % of the calculated value). So the field strength becomes 32 % higher than the design and the Kilpatrick coefficient becomes 1.49. The operation at the 1.5 MW was still stable and no severe discharge was experienced.

The designed maximum surface fields for the no.1 and the no. 2 tanks are less than that for the no.3 tank so that the high RF power operation of those cavities may not meet severe difficulty.

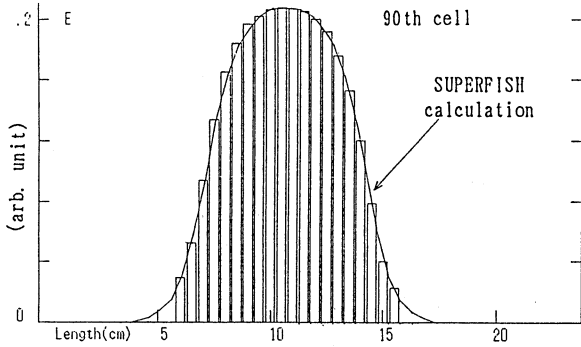


Fig.6 Field distribution in the 90th gap.

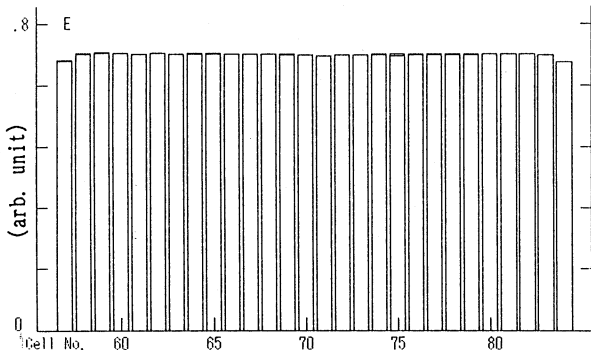


Fig.7 Field distribution for the no.2 tank after tuning.

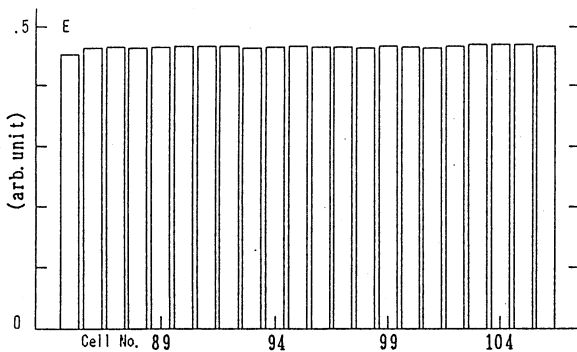


Fig.8 Field distribution for the no.3 tank after tuning.

RF control circuit performance

By the RF control circuit test, the same setup as the high RF power operation was used. Figure 9-(a) shows an RF waveform and an amplitude error signal and fig.9-(b) shows a feed back

signal and a phase error signal in a typical AGC and APC performance test with 1.2 ms and 950 kW RF pulse. An amplitude stability of 10^{-3} and a phase stability of 1 deg. were realized over 0.4 ms. This performance satisfies the condition required to the injector for stable operation of the HIMAC complex.

In the APC test done at the same time with those for the AGC and APC, the auto-tuners proved function well, keeping resonant condition of the cavity under operation, and overall performance of the APC system is satisfactory.

In view of good results obtained for the RF control circuits of the no.3 tank, RF tuning of the other cavities will not be very difficult.

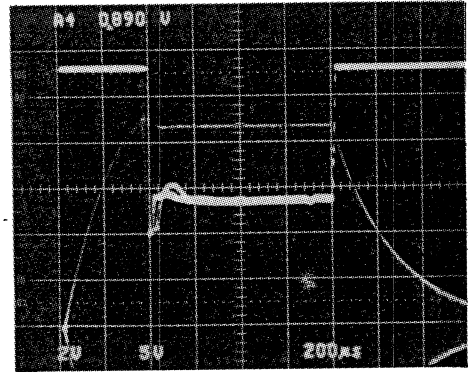


Fig.9-(a) RF waveform in the cavity and amplitude error signal.

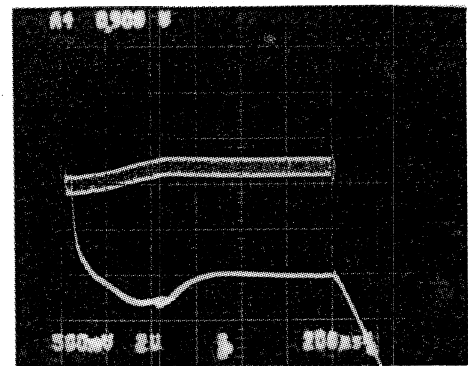


Fig.9-(b) APC feed back signal (upper) and phase error signal (lower, 9 deg./div).

Conclusion

Performance test of the HIMAC injector has been conducted at the SHI clean shop. By the test for RF characteristics of the Alvarez cavities, satisfactory results were obtained as follows;

1. In the tuning of the acceleration field and the resonant frequency, field uniformity within 3.5 % for the no.2 and 3 % for the no.3 tank was realized at 99.97 MHz.
2. By the high RF power operation for the no.3 tank, field strength higher than the design value by 32 % was sustained stably in the gaps.
3. The RF control circuit test proved to keep an amplitude stability of 10^{-3} and a phase stability of 1 degree over 0.4 msec in the 1.2 msec RF pulse.

Acknowledgment

We thank Dr.D.Böhne, Dr.J.Klabunde, and many GSI people for very useful discussions about the physical and engineering problems in the design stage of the HIMAC injector. We also gratefully acknowledge many helpful discussions with Dr.J.Staples.

References

1. Y.Sato, et al, Rev. Sci. Instrum. 61(1),466(1990)
2. A.Kitagawa, et al, Proceedings of this symposium.